**PAPER • OPEN ACCESS**

# Braking distance algorithm for autonomous cars using road surface recognition

To cite this article: C Kavitha *et al* 2017 *IOP Conf. Ser.: Mater. Sci. Eng.* **263** 062034

View the article online for updates and enhancements.

## Related content

- Methods of monitoring the technical condition of the braking system of an autonomous vehicle during operation
  A Revin, V Dygalo, G Boyko et al.

- Research on Brake System of Civil Aircraft
  Zijin Wang, Zhenshui Li and Wei Li

- Feasibility for the use of coal tar as a new material for road surfaces (pavement) construction
  M A Romero Farfán, H E Murillo Vega and F A Trujillo Pinto

## IOP ebooks™

Bringing you innovative digital publishing with leading voices to create your essential collection of books in STEM research.

Start exploring the collection - download the first chapter of every title for free.

# Braking distance algorithm for autonomous cars using road surface recognition

**C Kavitha[2], B Ashok[1], K Nanthagopal[1], Rohan Desai[1], Nisha Rastogi[1] and Siddhanth Shetty[1]**

[1]School of Mechanical Engineering, VIT University, Vellore - 632014, Tamil Nadu, India.

[2] Department of Electronics & Communication Engineering, Kumaraguru College of Technology (KCT), Coimbatore - 641049, Tamil Nadu, India.

Email id: ashok.b@vit.ac.in

**Abstract:** India is yet to accept semi/ fully – autonomous cars and one of the reasons, was loss of control on bad roads.  For a better handling on these roads we require advanced braking and that can be done by adapting electronics into the conventional type of braking. In Recent years, the automation in braking system led us to various benefits like traction control system, anti-lock braking system etc. This research work describes and experiments the method for recognizing road surface profile and calculating braking distance. An ultra-sonic surface recognition sensor, mounted underneath the car will send a high frequency wave on to the road surface, which is received by a receiver with in the sensor, it calculates the time taken for the wave to rebound and thus calculates the distance from the point where sensor is mounted. A displacement graph will be plotted based on the output of the sensor. A relationship can be derived between the displacement plot and roughness index through which the friction coefficient can be derived in Matlab for continuous calculation throughout the distance travelled. Since it is a non-contact type of profiling, it is non-destructive. The friction coefficient values received in real-time is used to calculate optimum braking distance. This system, when installed on normal cars can also be used to create a database of road surfaces, especially in cities, which can be shared with other cars. This will help in navigation as well as making the cars more efficient.

## 1.  Introduction

The main problems we face in India with respect to autonomous vehicles are poor quality roads (potholed), unpredictable road surface changes, variety and behaviour of traffic. Autonomous and semi-autonomous cars currently use default values of braking distance independent of road surfaces, and also drive at the speed limit when there are no slower vehicles in their path. Something that cannot be done in India was due to sudden and unpredictable changes in road surfaces. This project plans to solve one of the problems faced by autonomous cars by making a system for recognizing road surfaces and calculating braking distance. This system, when installed on normal cars can also be used to create a database of road surfaces, especially in cities, which can be shared with other cars. This will help in navigation as well as making the cars more efficient. An autonomous car is a vehicle that is capable of sensing its environment and navigating without human input. Many such vehicles are being developed, but as of now automated cars permitted on public roads are not yet fully autonomous. They

all require a human driver at the wheel who is ready at a moment's notice to take control of the vehicle. Autonomous cars use a variety of techniques to detect their surroundings, such as radar, laser light, GPS, odometer and computer vision. Advanced control systems interpret sensory information to identify appropriate navigation paths, as well as obstacles and relevant signage. Autonomous cars have control systems that are capable of analyzing sensory data to distinguish between different cars on the road, which is very useful in planning a path to the desired destination. Some demonstrative systems, precursory to autonomous cars, date back to the 1920s and 1930s. The first self-sufficient (and therefore, truly autonomous) cars appeared in the 1980s [1-3].

A major milestone was achieved in 1995, with CMU's NavLab 5 completing the first autonomous coast-to-coast drive of the United States. Of the 2,849 miles between Pittsburgh, PA and San Diego, CA, 2,797 miles were autonomous (98.2%), completed with an average speed of 63.8 miles per hour (102.3 km/h). Since then, numerous major companies and research organizations have developed working prototype autonomous vehicles. Among the potential benefits of autonomous cars is a significant reduction in traffic collisions; the resulting injuries; and related costs, including a lower need for insurance. Autonomous cars are also predicted to offer major increases in traffic flow; enhanced mobility for children, the elderly, disabled and poor people; the relief of travelers from driving and navigation chores; lower fuel consumption; significantly reduced needs for parking space in cities; a reduction in crime; and the facilitation of different business models for mobility as a service, especially those involved in the sharing economy [4-6]. The friction coefficient of a tire is based on the general theory of friction. The friction coefficient of a tire varies with the amount of skidding or spinning of the tire. 100% skidding means the wheel is locked while the vehicle is moving (a situation similar to the tire moving sideways) and 100% slipping means the wheel is rotating while the vehicle is not moving. Under these situations, there is a relative motion between the road and the tire; hence it is under kinetic friction (or sliding). Peak values for the friction coefficient of a tire happen around 20% skidding (or slipping) and may be related to static friction.

The current practice of measuring the displacement of a vehicle body often uses linear variable differential transformers (LVDT) under stationary conditions.  This kind of direct measurement technique has limitations in that it is very difficult to be used on a road test if not impossible.  Another way to directly measure displacement is with a laser displacement gauge, which can accurately measure very small displacements.  However, the equipment is very expensive and not suitable for a road test either.  It requires a fixed point of reference to function properly, meaning that the laser head making the measurements must be positioned within a certain distance away from the object [7,8]. Therefore, there is a need for a reliable measurement technique that can be used on a road test.  One potential technique is to use an accelerometer to measure acceleration, which can then be converted into displacement.  The three quantities i.e. position, velocity, acceleration is interrelated through integrals and derivatives.  This indirect method of measuring displacement would solve the need for a fixed reference.  Acceleration based displacement methods are categorized as inertial based measurement techniques in contrast to the direct measurement methods, which are grouped into reference point techniques. Unfortunately, India still does not have the requisite infrastructure conducive to the use of autonomous technology. There are multiple factors on Indian roads, which the autonomous car will have to consider, apart from the usual parameters, such as – unpredictability of road users, non-compatibility of navigation software with certain roads, ever changing road conditions, unpredictable changes in road surface, etc. This project focuses on the issue concerning road surfaces and therefore, the vehicle's braking distance. The road surface can be mapped using a ranging sensor which has moderate to high accuracy. Ultrasonic sensor has been used as it provides a good balance between accuracy and cost effectiveness. Ultra-sonic sensors are already used in vehicles for parking assist to avoid accidents in the parking lot, the transmitter in the sensor send signals and the receiver receives the signal that has be bounced back and calculates the distance of the obstacle from the rear end of the vehicle, it warns the driver accordingly. Similarly, an ultrasonic sensor can perform a contactless measurement of the distance between road surface and vehicle body. The measurement of distance without contacting the target is done by generating 40 kHz ultrasonic waves

using ultrasonic transducers. Here the distance is calculated on the basis on time taken by the pulse generated by the ultrasonic transducer to travel to the target and return as reflected echo. This device also makes the use of microcontroller for calculating the distance and displaying it on a seven-segment display. The distance up to 2.5m is calculated in air medium at ambient temperature [9-12].

Pavement roughness is generally defined as an expression of irregularities in the pavement surface that adversely affect the ride quality of a vehicle (and thus the user). Roughness is an important pavement characteristic because it affects not only ride quality but also vehicle delay costs, fuel consumption and maintenance costs. Measurement of roughness is indicated in terms of cumulative measure of vertical displacements as recorded by a recording wheel due to the unevenness in the longitudinal profile of the road. This cumulative measure of ups and downs in road profile is termed as roughness index or unevenness index and is normally represented in m/km or mm/km. The roughness of the road surface constitutes the smoothness, and frictional properties of the pavement surface and in turn related to the safety, and the ease of the driving path. The roughness of a pavement is an important parameter in determining the comfort level of the riding path on a pavement, and this roughness of the pavement surface is related to the vehicle vibration, operating speed, wear and tear of the wheels. The surface roughness of a pavement is determined using the international roughness index (IRI), which is a measure of the texture of a pavement surface. Within this context, the current research work focuses on braking distance measurement and the experimental method for recognizing road surface profile and calculating braking distance.

## 2. Methodology

### 2.1 Stopping distance

The stopping distance while braking the vehicle is given by the following relation,

$$d = \frac{1}{2K_a} \ln \left( 1 + \frac{K_a}{K_t} v^2 \right) \tag{1}$$

$$K_a = \frac{\rho}{2m} (C_D) \tag{2}$$

$$K_t = (0.01 + \mu)g \tag{3}$$

Where

$\rho$   = atmospheric air density (= 1.225 kg/m³)

$C_D$ = Drag factor

$C_L$ = Lift factor

$m$ = vehicle mass

$g$ = gravitational = acceleration (= 9.80665 m/s²)

$\mu$ = tire-road friction coefficient

$f_r$ = rolling resistance coefficient

The above formula is used to calculate the braking distance of a vehicle, this can be converted as a base formula for the MATLAB software to follow every time it receives data from the Arduino as a sensor output. This can be done by connecting the Arduino board to the ultrasonic sensor which gives the data to the Arduino which is the displacement values with respect to time. The stopping distance also depends on Drag coefficient and air properties like air density in a relation as shown in (2). Finally, the braking distance can is calculated by considering all the factors that affect the velocity of the vehicle through the equation (1).

*2.2. Preparation of code*

The project uses Arduino in tandem with MATLAB to process the data obtained from the sensor. Two separate codes need to be used for the same. One is an Arduino code, while the other is the MATLAB code. The Arduino code is used to obtain data from the ultrasonic sensor and convert it to

displacement values, which can be used in MATLAB to further process it. The distance is calculated in centimetres. The MATLAB code obtains the displacement data from the Arduino. This data is divided into sets of 16. Standard deviation of each set is obtained, which is a measure of the roughness of that particular stretch of road. This roughness is converted to friction coefficient using a constant which is specific to the type of tyres being used. The friction coefficient of a tire is based on the general theory of friction. The friction coefficient of a tire varies with the amount of skidding or spinning of the tire. 100% skidding means the wheel is locked while the vehicle is moving (a situation similar to the tire moving sideways) and 100% slipping means the wheel is rotating while the vehicle is not moving. Under these situations, there is a relative motion between the road and the tire, hence it is under kinetic friction (or sliding). Peak values for the friction coefficient of a tire happen around 20% skidding (or slipping) and may be related to static friction.

Generalizing, a different constant needs to be used for soft, medium and hard compound tyres. We substituted a value for a common medium compound tyre like Bridgestone B250, or Michelin XM Earth1. The vehicle chosen for the default values was a Toyota Etios with a kerb weight of 1000 kg, and drag coefficient of 0.295. The default speed was taken as 100 km/h, or this was changed accordingly to test the code at different speeds, as can be seen in the graphs.
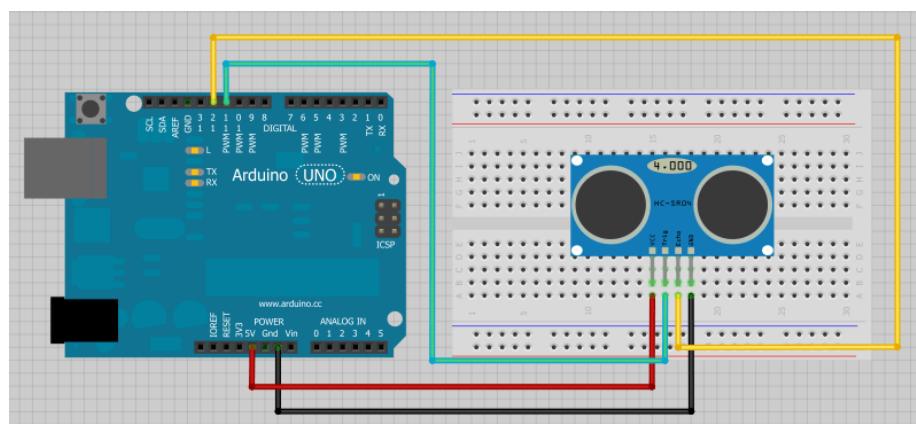
*2.3. Arduino Circuit & Code*



**Figure 1.** Ultra- sonic sensor circuit

Seen in Figure 1, the Ultra-Sonic sensor consists of four pins Vcc, Gnd, Trigger and Echo in which the Trigger pin is connected to 12 pin of the Arduino (Digital pin) and Echo pin is connected to 13 of the Arduino, a delay time of 100 micro seconds are provided to get a continuous outputs from the sensor. The sensor calculates the time taken by the wave to rebound and then plots the displacement from the sensor. As the output is to be converted to centimetres we introduce a character with value of 10000 in the code and the baud rate to 9600 bits per second for serial output for data transmission. Initially it is made sure that the trigger is not transmitting and signal. To do so it is turned into low/off mode for 10 micro seconds. Trigger pin is given a 10 micro Second length of the HIGH pulse, at this point the ECHO pin goes to HIGH until it receives the reflected signal. The Trigger pin send the signal

and the echo pin receives after rebound of the wave and it calculates the distance travelled from the formula and then plotted on the serial monitor after every 10 micro seconds.

*2.4 Prototype*

A mechanical working prototype is manufactured using a double A-arm suspension and with a frame to mount on the wheel is shown in Figure.2. The electronic equipment like Ultra-Sonic sensor and Arduino Uno board as well as a laptop to continuously plot the displacement values.
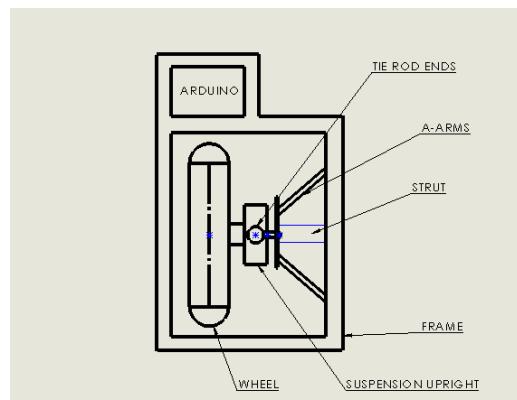


**Figure 2.** 2D model of experimental setup

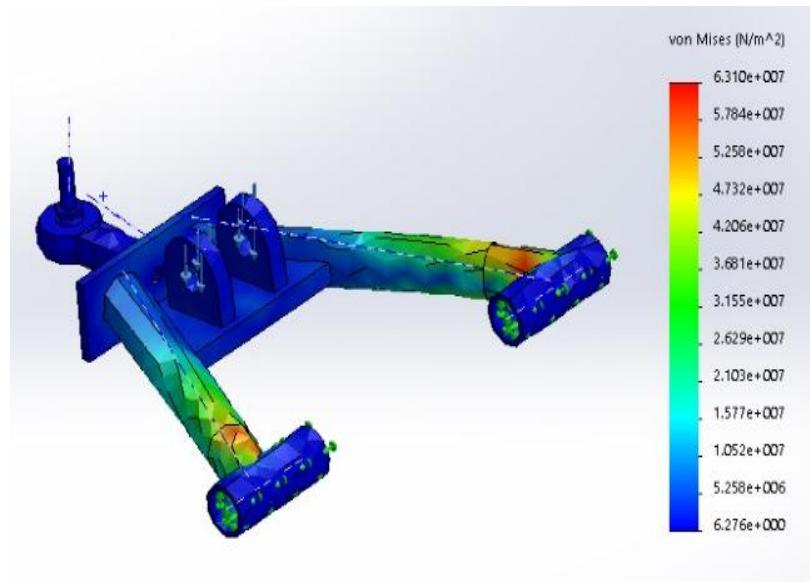*2.4.1 Design of double A-arm Suspension*

**Figure 3.** Various views of CAD model design

A double a-arm suspension is made using a 1-inch diameter cast iron rods and bike rear suspension strut to make a model of a vehicle suspension system. The main reason for using a suspension is to reduce vibrations for the electronic equipment on the frame so that the Ultra-sonic sensor results were much reliable. The spring coefficient of the strut is 47 N/mm and the maximum suspension travel is 50mm on full compression. The Figure 3 resembles the quarter car model of a car with a double a arm suspension with a metallic frame made by the 1in square hollow rods to resemble the chassis of the vehicle, this quarter car model has an additional frame that is in front of the tire to accommodate the electronic equipment like Arduino and sensors on a bread board. The sensor is mounted on the bread board and is calibrated according to the initial surface profile and later on the Arduino generates a mean deviation continuously and find the displacement.

*2.4.2. Static analysis of the lower A-arm.* The lower arm must bare more loads as well as the reaction forces by the knuckle and must bear the un-sprung mass of the vehicle which is the weight of tyre, disc brakes and callipers and axle (if any). These loads are totally 2500N, as can be seen from Figure 4. It also includes the weight of the strut that is connected to the chassis/frame which dampens the vibration. The load of the strut will be acting on the mounting points on the lower arm. The deflection of the both the a-arms are acceptable due to a very less deflection observed, as the load applied on them is one quarter of the weight of the vehicle. The strain of the system is very low because of the lower deflection when compared to the total length of the body and the results are shown in Table.1.
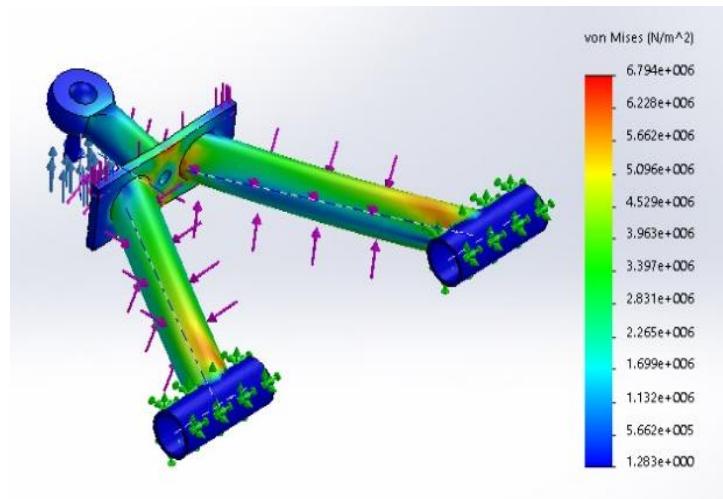
**Table 1.** Lower a-arm analysis results

| Name | Type | Min | Max |
|------|------|-----|-----|
| Stress | Von missus stress | 0 N/m^2 | 3.6389e+007 N/m^2 |
| | | Node: 19281 | Node: 14008 |
| Displacement | Resultant Displacement | 0 mm | 0.834921 mm |
| | | Node: 3317 | Node: 141 |
| Strain | Equivalent Strain | 0 | 0.000430089 |
| | | Element: 10563 | Element: 7610 |

**Figure 4.** Von misses stress of lower a-arm

*2.4.3. Analysis of upper A-arm.* The Figure 5 shows the deflection of upper a-arm of the suspension system with all the possible loads applied on it, the deflection of the a-arm are acceptable due to a very less deflection observed, reaction force is acted upon the upper arm this reaction force is due to the upright and this reaction force is nearly equal to the un-sprung mass of the suspension assembly which is nearly 70N, this force is applied opposite to weight of the model, whereas on the lower arm this reaction force is downwards i.e., it is added to the weight of the model. The minimum deflection is seen at the end of a-arms which are connected to the frame (blue coloured) and the maximum deflection is seen at the ball joint end as most of the forces are acting near it. Since the loads acting on both of the arms are different, it can be seen that the lower arm has deflected more than upper arm and also have lower von misses stress than which can be observed in Table 2.

**Table 2.** Upper A-arm analysis results

| Name | Type | Min | Max |
|---|---|---|---|
| Stress | Von missus stress | 1.28265 N/m^2<br>Node: 19270 | 6.79424e+006 N/m^2<br>Node: 16363 |
| Displacement | Resultant Displacement | 0 mm<br>Node: 6536 | 0.0523636 mm<br>Node: 4107 |
| Strain | Equivalent Strain | 5.88678e-012<br>Element: 3681 | 2.4867e-005<br>Element: 9185 |

**Figure 5.** Von misses stress of upper a-arm

*2.4.4. Analysis of the Upright.* On the upright, most of the loads are acted on the bottom part where the lower arm is fixed as shown Figure 6. Another force which is applied on the knuckle/upright is to steer the upright to turn the vehicle, this force will be acting perpendicular to the plane of the knuckle. Most of the forces that are acting on the upright are damped before it affects the chassis of the vehicle. Many of the reaction forces are negated by the reactions forces as well as the additional forces like the un-sprung weight of the vehicle which also creates forces on the suspension system. As seen in the Figure 7, the maximum von misses stress acting defines the existing stress is less than the yield strength of the material. So, the upright doesn't fail for the loads we applied and the analysis result is listed in Table 3.

**Table 3.** Up right analysis results

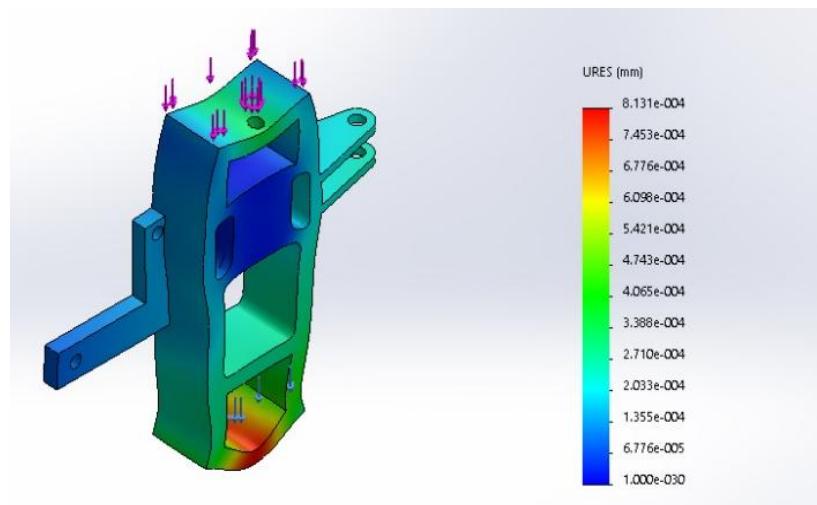| Name | Type | Min | Max |
|------|------|-----|-----|
| Stress1 | VON: von Mises Stress | 0.15005 N/m^2 Node: 849 | 2.6827e+006 N/m^2 Node: 119 |
| Displacement1 | URES: Resultant Displacement | 0 mm Node: 39 | 0.000813076 mm Node: 16818 |
| Strain1 | ESTRN: Equivalent Strain | 7.42056e-013 Element: 1618 | 7.32512e-006 Element: 5628 |

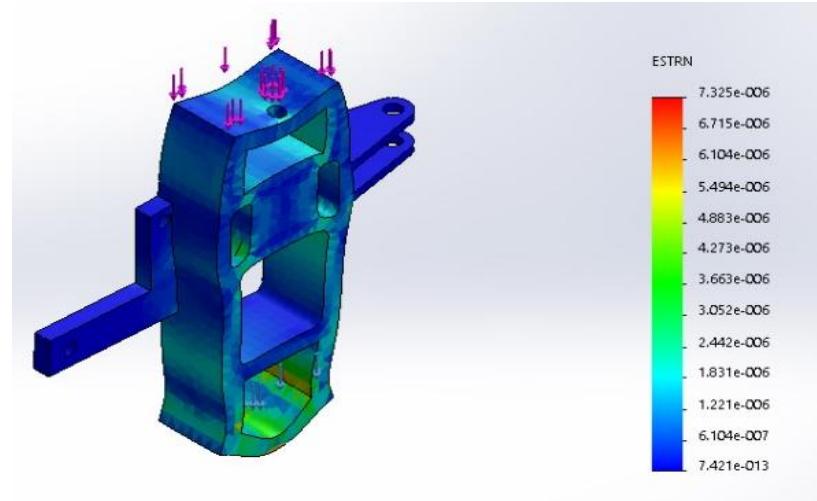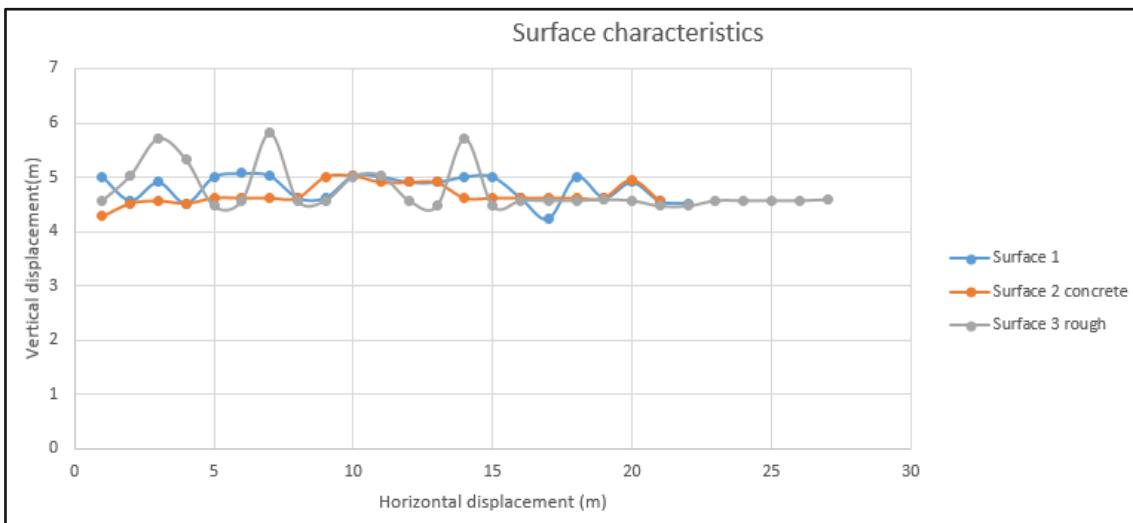**Figure 6**. Displacement analysis of upright



**Figure 7.** Von misses stress analysis of upright

## 3. Results and discussion

The performance of the ultrasonic sensor and braking distance algorithm were tested on 3 different surfaces, and one simulated road profile using a quarter car model prototype. The displacement, roughness, friction coefficient and braking distance results were plotted, analysed and compared. Moreover, braking distances were compared for one surface using different velocities, and friction coefficient was compared for one surface for different compounds of tyres.
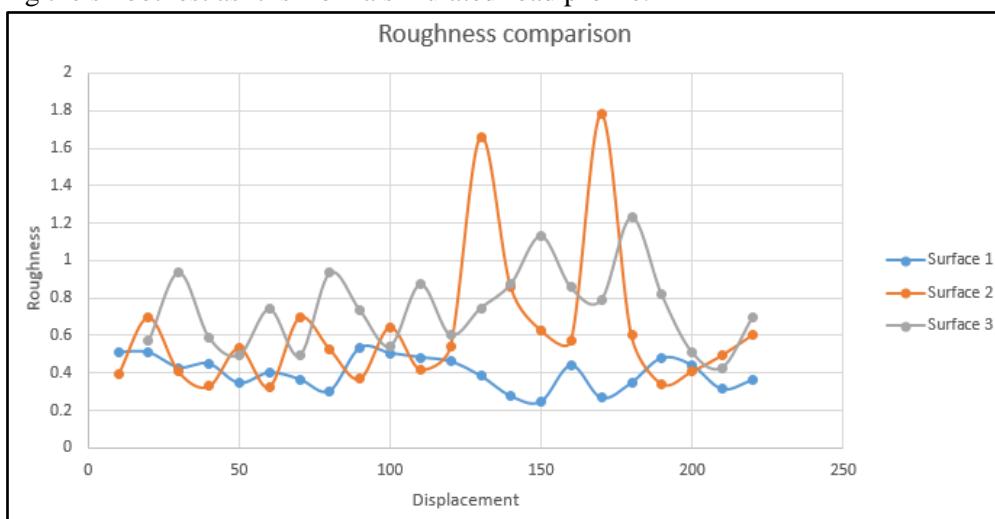
### 3.1 Surface characteristics

The plot in Figure 8 shows the direct output from the sensor in centimetres. Three different surfaces have been shown which were tested, surface 1 were being a sample road profile generated using White Gaussian Noise in MATLAB, surface 2 a concrete street, and surface 3 an unevenly paved street with potholes. As can be seen from the graph, surface 3 (Grey) has the most undulations and thus has a higher standard deviation. The peaks are the points on the road with potholes. On the other hand, the concrete surface (Orange) has the least undulations, which is in keeping with it being the smoothest of the three.
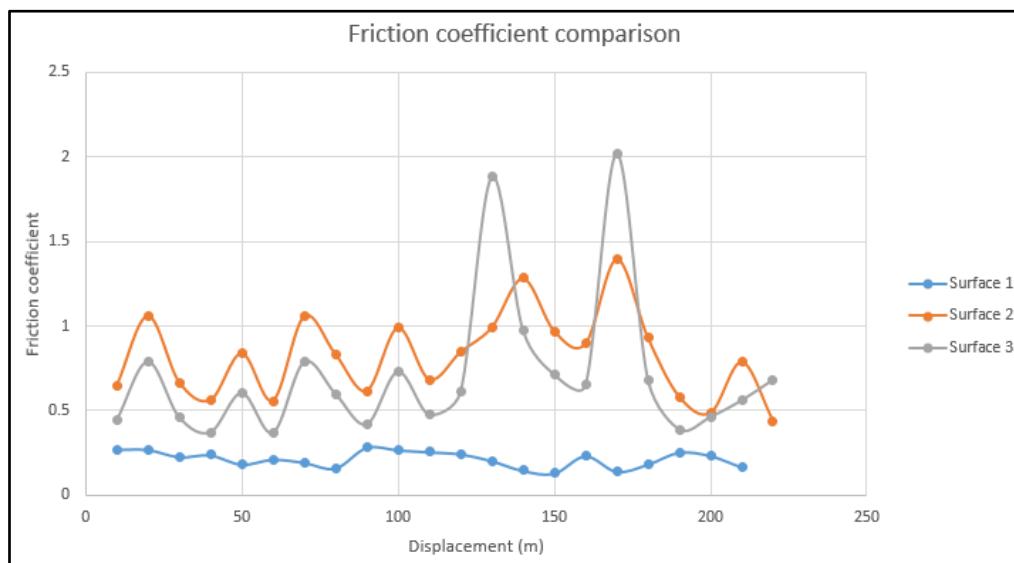
**Figure 8**. Surface characteristics Vs displacement

### 3.2 Roughness characteristics Vs Displacement

The plot in Figure 9 shows the roughness characteristics for the 3 surfaces tested. The roughness here is measured in cm/m. These values are the standard deviation values of sets of 16 values out of a total of 256, obtained from the sensor plot. The peaks of 1.65cm/m and 1.8cm/m in the Orange plot show that the road surface is relatively rougher at these points, or in other words, uneven. The valleys before these 2 points bring out the unpredictability in the road conditions that were pointed out in the introduction. The road suddenly changes from smooth to uneven. And it is exactly this is a hindrance to autonomous vehicles. Similar trends are observed in the graphs of the other 2 surfaces, the blue graph being the smoothest as it is from a simulated road profile.



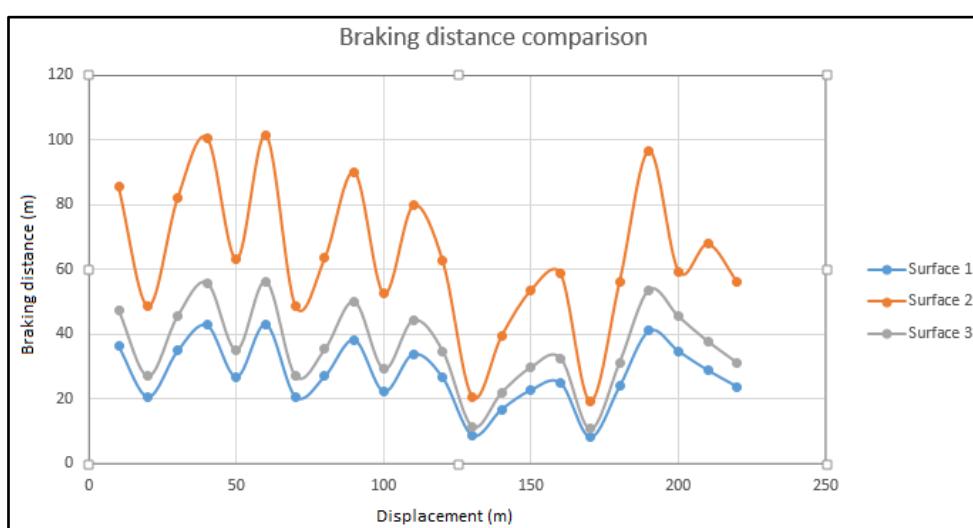**Figure 9.** Roughness index vs Displacement

### 3.3 Friction coefficient Vs Displacement

**Figure 10**. Friction coefficient Vs Displacement

The plot in Figure 10 shows the variation of friction coefficient between the tyres and the surface, against the displacement of the vehicle. The friction coefficient is found to be erroneously high at 2 points in the graph. This can be attributed to the sensor showing anomalous values. Apart from those points, the plots for concrete (Orange) and rough tarmac (grey) are seen to fluctuate between 0.5 and 1, which is normal. These plots are for a commonly used Medium to Hard compound tyre used in mass market cars in India – like the Bridgestone B250 and Michelin XM Earth1.

*3.4 Braking distance comparison*
The plot in Figure 11 (a) shows the braking distance comparison at a default speed of 100km/h for the different surfaces tested. Surface 2 (Orange) is the simulated profile and hence the values here are the furthest from actual as the road appears to be extremely smooth with a low coefficient of friction. Surface 1 and Surface 3 generate more realistic coefficients of friction and therefore the braking distances are close to reality. The braking distances for the 2 plots range from 30-55m. Stopping distances (100kph-0) for midsize sedans like the Etios, Hyundai Verna and Honda Civic range from 40-55m.



**Figure 11 (a).** Braking distance comparison Vs Displacement
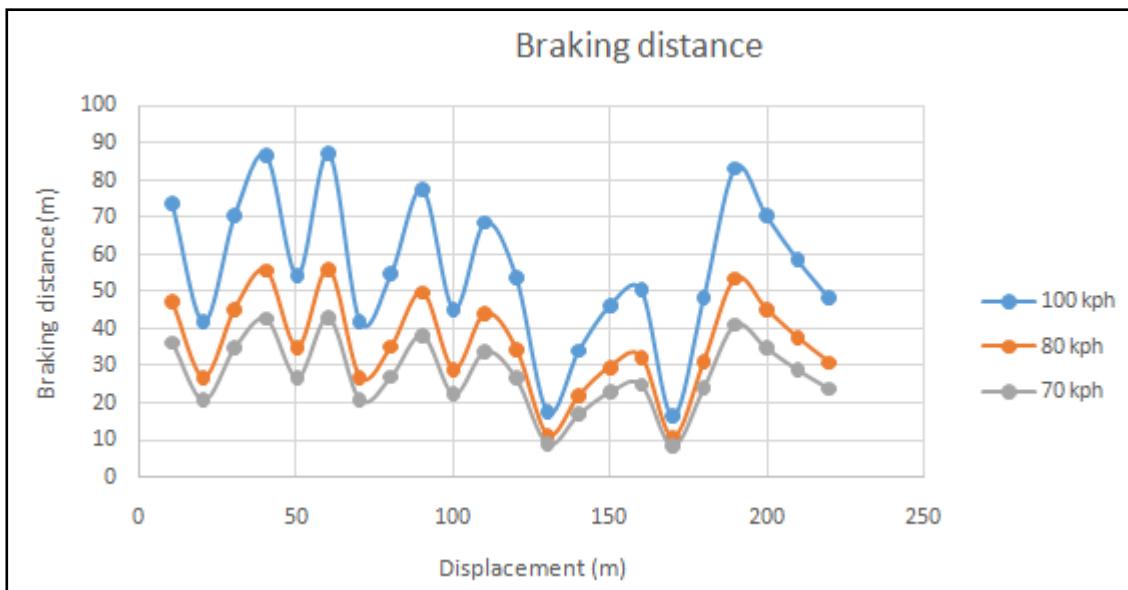
*3.4.1. Braking distance (Speed comparison)*



**Figure 11 (b).** Braking distance (Speed comparison)

The following plot in Figure 11 (b) shows the variation of braking distance with variation in friction coefficient, at speeds of 70 km/h, 80 km/h and 100 km/h. Also attached is another graph which elucidates the inverse relationship between friction coefficient and braking distance. As friction coefficient increases, braking distance decreases. The peaks are due to points of low friction coefficient on the road surface; these could be extremely smooth patches of road, while the dips are due to uneven, potholed surfaces.

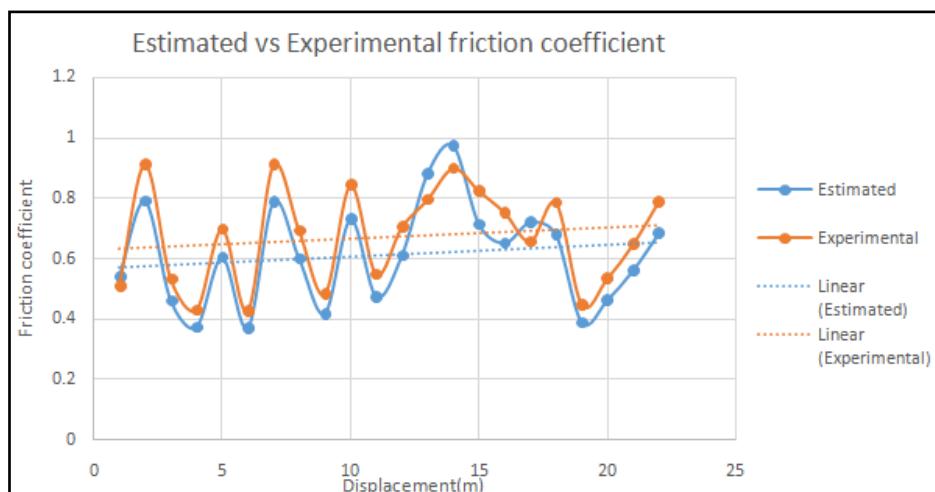*3.4.2. Friction coefficient comparison*



**Figure 12.** Friction coefficient comparison estimated

The plot in Figure 12 shows the comparison between the estimated friction coefficient for a surface and the experimentally observed friction coefficient of the surface. The mean of the values obtained for both is calculated and can be seen as the trend lines plotted in the graph. The mean difference between the estimated and experimental friction coefficient was found to be 0.052, which is a difference of 7% from the estimated value (<10%).

## 4. Conclusion

This project was undertaken with the objective of easing the integration of autonomous vehicles on Indian roads. The main aim of this project was to come up with a solution for autonomous vehicles to map the road profile continuously and calculate friction coefficient using the roughness of the road. A sample vehicle was taken to decide certain values which would be kept as default in the code for calculating braking distance eventually. Toyota Etios was chosen as the sample vehicle, with a kerb weight of 1000kg, and drag coefficient of 0.295. The displacement plot from the ultrasonic sensor was used to find roughness using standard deviation. A constant was obtained, which is specific to tyre compounds to convert this roughness to friction coefficient. Rough surfaces gave high friction coefficient values while smoother surfaces, lower. The values obtained for the braking distance on smooth tarmac surface were consistent with the actual values of braking distance for the car. Estimated and experimental friction coefficients and braking distances were observed. The deviation was found to be 7% for the friction coefficient, while it was found to be a maximum of 8% for the braking distance.

## References

[1]   Ashok, B., Ashok, S.D. and Kumar, C.R., (2016). *A review on control system architecture of a SI engine management system.* Annual Reviews in Control, 41, pp.94-118.

[2]   Kwang H J, Morosiuk G and Emby J, *Assessment of skid resistance and macrotexture of bituminous road surface in Malaysia.* Seventh REAA conference, Singapore 443-449.

[3]   Ashok, B., Ashok, S.D. and Kumar, C.R., (2017). *Trends and future perspectives of electronic throttle control system in a spark ignition engine*. Annual Reviews in Control. (In Press).

[4]   Fambro DB, Fitzpatrick K and Koppa R (1997), *A new stopping sight distance model for use in highway geometric design*. Transportation Research Circular Transportation Research Board, National Research Council, Washington D.C.

[5]   Hernan de Solminihac Marcelo Bustos Thomas Echaveguren, *Development of Correlation equations between different measurements of skid resistance in pavements*, Indian Journal of Engineering and Material Sciences.

[6]   H He and J Liu, *The design of ultrasonic distance measurement system based on S3C2410*, Proceedings of the IEEE International Conference on Intelligent Computation Technology and Automation, Oct. 2008, pp. 44-47.

[7]   Y Jang, S Shin, J W Lee, and S Kim, *A preliminary study for portable walking distance measurement system using ultrasonic sensors*, Proceedings of the 29th Annual IEEE International Conference of the EMBS, France, Aug. 2007, pp. 5290-5293.

[8]   Masaru Sugai, Hiroyuki Yamaguchi, Ndnori Miyashita, *New Control Technique for Maximizing Braking Force on Antilock Braking System*. Vehicle System Dynamics,32(1999), pp.299-312

[9]   Alvarez L, Yi J, Clarys X and Horowitz R, *Emergency braking control with an observer-based dynamic tire/road friction model and wheel angular velocity measurement*, Vehicle System Dynamics, 2003, 39, (2), pp.81-97.

[10]  Wang Run-qi, Jian ju, *Analysis and Calculation of Braking Distance of ABS Automobiles,* Journal of Central South Forestry University, 2005, 25(2):pp.12-14.

[11]   D Webster, *A pulsed ultrasonic distance measurement system based upon phase digitizing*, IEEE Transaction on Instrumentation and Measurement, Vol. 43, No. 4, Aug. 1994, pp. 578-582.